Mechanical Engineering Research; Vol. 6, No. 2; 2016
ISSN 1927-0607 E-ISSN 1927-0615
Published by Canadian Center of Science and Education

Mathematical Modelling and Control of a Two-Wheeled PUMA-LikeVehicle

Khaled M Goher[1]

[1] Department of Informatics and Enabling Technologies, Lincoln University, New Zealand

Correspondence: Khaled M Goher, Department of Informatics and Enabling Technologies, Lincoln University, New Zealand. E-mail: Khaled.Goher@lincoln.ac.nz

Received: September 26, 2016 Accepted: October 15, 2016 Online Published: November 23, 2016

doi:10.5539/mer.v6n2p11 URL: http://dx.doi.org/10.5539/mer.v6n2p11

Abstract

This paper presents mathematical modelling and control of a two-wheeled single-seat vehicle. The design of the vehicle is inspired by the Personal Urban Mobility and Accessibility (PUMA) vehicle developed by General Motors® in collaboration with Segway®. The body of the vehicle is designed to have two main parts. The vehicle is activated using three motors; a linear motor to activate the upper part in a sliding mode and two DC motors activating the vehicle while moving forward/backward and/or manoeuvring. Two stages proportional-integral-derivative (PID) control schemes are designed and implemented on the system models. The state space model of the vehicle is derived from the linearized equations. Controller based on the Linear Quadratic Regulator (LQR) and the pole placement techniques are developed and implemented. Further investigation of the robustness of the developed LQR and the pole placement techniques is emphasized through various experiments using an applied impact load on the vehicle.

Keywords*:* PUMA, Inverted pendulum, PID, LQR, Pole Placement

1. Introduction

The research on balancing two-wheeled robots has gained momentum over the last decades worldwide in robotics laboratories. This is due to the inherent unstable dynamics of such systems. The control quality of such robots is characterized by the ability to balance on its two wheels. This additional manoeuvrability allows easy navigation on various terrains, turn at sharp corners and traverse small steps or curbs. These capabilities have the potential to solve a number of challenges in the industrial and public sectors. Small carts built utilizing this technology allow humans to travel short distances in a confined place as opposed to using cars or buggies.

Segway, shown in Figure 1, is a famous two-wheeled balancing robot which is currently used as a commercial human transporter. Segway uses gyroscopes and tilt sensors to keep the rider in the upright position. Additional sensors are used for safety precautions. Browning et al. (2004) presented a new domain, called Segway Soccer, for investigating the coordination of dynamically formed, mixed human-robot teams within the realm of a team task.

General Motors® (GM) and Segway® have developed the Personal Urban Mobility and Accessibility (PUMA); shown in Figure 2, as an electrically powered two-seat vehicle with only two wheels. PUMA is a self-balancing 300 lb (136 kg) two-wheeled vehicle that can travel up to a speed of 35 mph for 8-10 hours for each single charge of the battery. PUMA is equipped by a lithium battery as well as vehicle-to-vehicle communications system for reducing the risk of accidents and regulating the flow of traffic. This vehicle represents a solution to the world's urban transportation problems while affording the advantages of being a fast, safe, inexpensive and a clean alternative compared to traditional cars and trucks.

As similar innovations of compact personal transportaions; Laurent et al (2010) developed a compact two-wheeled vehicle B2 transportation system, shown in Figure 3, which is able to move in narrow city streets. B2 has similar functions to Segway human transporter. However, the control objectives are different due to the difference in the intended use of each vehicle.

The Segway behaves like an inverted pendulum (e.g. when a driver leans forward, the Segway accelerates forward to prevent the passenger from falling), whereas the task of B2 will be to balance the occupants while rejecting the influence of the road and passengers. Thus, the passenger motion is considered as a disturbance which needs to be rejected. Furthermore; the B2 is considered as an alternative road vehicle not only for sidewalks.

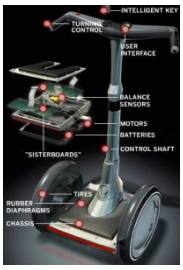

Figure 1. Segway human transporter Figure 2. PUMA prototype

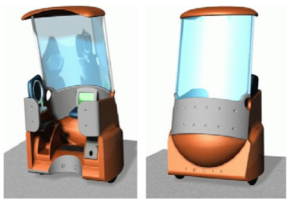

Figure 3. B2 urban transportation system

2. Related Work: Control Strategies of Two-Wheeled Machines

Various control strategies have been proposed by numerous researchers to control the two-wheeled machines. Salerno and Angeles (2004) developed multivariable differentiable state feedback control to stabilizable two-wheeled quasi-holonomic robots. The analysis of robot stability, based on the Lyapunov linearization method has been provided. Tinkir et al. (2010) presented a comparison of a PID control and Interval type-2 fuzzy logic control (IT2FL) of a double inverted pendulum system. A fast convergence stable response has been achieved with the IT2FL controller. However, the system showed an unstable response with the PID controller. Jingato et al. (2008) used a PID controller combined with neural networks to stabilize a two-wheeled robot. Tatikonda et al. (2010) applied an ANFIS controller on an inverted pendulum (IP) system using different payloads. Han et al. (2010) developed a self-adaptive fuzzy PID with three double-input single-output fuzzy controllers for an IP system. Although the system was fast in reaching stability, it was accompanied with oscillations.

Harrison (2003) implemented a near optimal, non-linear controller based on linear quadratic (LQ) optimal control theory on a single IP on a cart. The resulting regulator could be implemented in real-time. However, the need to solve an algebraic Riccati equation at every time-point is burdensome. Lin et al. (1996) proposed a linear state feedback controller to balance an IP based on combining a low gain and high gain state feedback. Bugeja (2003) developed a state feedback pole-placement controller to swing-up and stabilize an IP system using a cascade control loop. Fiacchini et al. (2006) presented various controller types for both linear and non-linear control mechanisms including: partial linearization, energy shaping, velocity stabilization and non-linear controller tuning on a personal IP vehicle. Bogdanov (2004) applied different optimal controllers on a double IP system. Linear Quadratic Regulator (LQR), state-dependent riccati equation (SDRE) and optimal neural network controllers have been compared. Xiong et al, (2010) presented a new method to find the parameters of an optimal LQR controller for a double IP system. Optimal selection of the LQR controller parameters was superior and tended to equilibrium point faster than heuristic selection of the parameters. Wongsathan and Sirima (2009) applied genetic algorithm (GA) to design an LQR controller for the IP system. Nasir et al, (2010) presented a comparison between LQR and PID-controller for a two-wheeled robot in terms of input tracking and the capability of disturbances rejection. Nawawi et al (2006) proposed a robust controller based on sliding mode control for stabilization and disturbance rejection.

2.1 Paper Contribution

In this paper; the authors presented a two-wheeled single-seat vehicle. The design of the vehicle is inspired by the Personal Urban Mobility and Accessibility (PUMA) vehicle developed in 2009 by General Motors® in collaboration with Segway®. An investigation of the system model performance is carried out based on the linear state space model. The control of the system is carried out using LQR and pole placement techniques. The robustness of the control algorithms is tested against external disturbance.

2.2 Paper Overview

This paper is organized as follows: Section 3 describes the system model, the different modes of operation and the governing dynamic equations based on lagrangian formulation. In Section 4; PID control is implemented on the nonlinear model of the vehicle as well as the state space linear model of the vehicle which is developed where LQR and pole assignments are used to control the system model. The paper is concluded in Section 5 highlighting the achievements of the work and proposed recommendations for future work.

3. Description Modelling of the System

3.1 System Modelling

The system is comprising two main parts; a lower part holding the main wheels, motors and cluster wheels and the upper part carrying the user and the top parts of the vehicle. The model of the system is simplified in this work for three modes of operation (parking mode, sliding of the upper part and stabilization of the entire system) comprising the entire motion of the vehicle. The vehicle is activated by two motors attached to the main wheels and a linear actuator for the sliding of the upper part. The system has three degrees of freedom (DOF); forward/back linear motion of the entire system, angular oscillation around the vertical upright position and a linear displacement of the upper part of the vehicle. The system is designed in SolidWorks with the numerical parameters given in Table 1. The dynamic model of the whole system consists of two separate mathematical models describing the sliding mode and the stabilization mode. The entire motion of the system can be described by the following three successive modes:

- ***Stage 1 (parking mode)***: The system is parking during this stage. The upper part is not activated by the linear actuator and the entire vehicle is inclined relative to the vertical position. The vehicle at this stage stands on the two main wheels and two cluster wheels, Figure 5(a). No actuation from any of the motors or the linear actuator is needed at this stage.
- ***Stage 2 (sliding mode)***: once the linear actuator starts working; the upper part will slide along the lower base with a linear displacement (y) while the entire vehicle is still inclined relative to the vertical position. The linear actuator has to apply a linear force F_L sufficient to push the upper part to the desired position. A locking mechanism will lock the upper part in place at the end of the linear stroke so that the actuator can get dis-engaged. A simplified schematic representation of this mode is shown in Figure 6. The vehicle is shown in Figure 5(b) at the end of this stage.
- ***Stage 3 (stabilization mode)***: The stabilization mode is taking action between stages 2 and 3 where the two motors, activating the wheels, work together in order to lift the vehicle from stage 2 and to balance the entire system at stage 3. By the end of this stage; the entire system has to be erected and stabilized in a vertical upright position while the wheels have limited forward and back motion. The system in the stabilization upright position is shown in Figure 5(c).

Table 1. Vehicle numerical parameters and description

Terminology	*Description*	*Value*	*Units*
L_r	Rod length	0.7	m
M_r	Rod mass	1	kg
M_c	Total cart mass	145	kg
R_w	Wheel radius	0.25	m

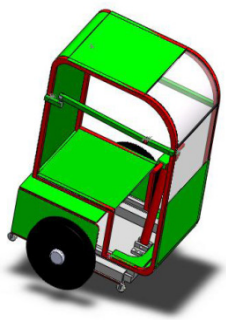

Figure 4. SolidWorks design of the system

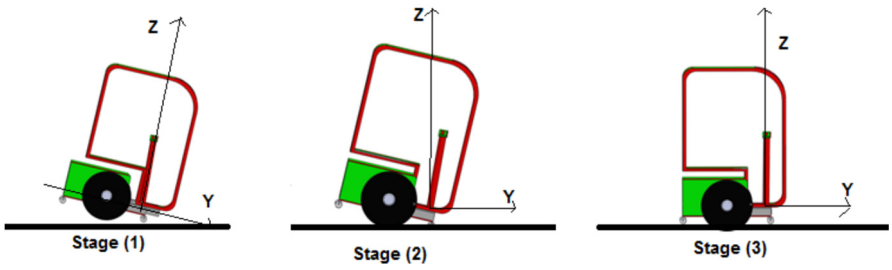

(a) (b) (c)

Figure 5. Schematic diagram showing the stages of motions

3.1.1 Sliding Mode

Lagrangian-Euler (LE) dynamic approach is used to drive the equations of motion of the upper part of the vehicle. The upper part is simplified by a single mass sliding on a plane with an inclination angle φ as shown in Figure 6. This sub-system is a one degree of freedom with the linear force developed by the linear actuator as the input and the linear displacement y as the output.

Appling Lagrangian dynamic formulation on the sliding part yields the following equation:

$$\frac{d}{dt}\left(\frac{\partial L}{\partial \dot{y}_i}\right) - \frac{\partial L}{\partial y_i} = F_L \tag{1}$$

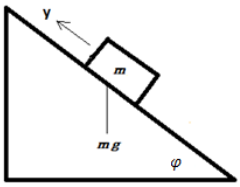

Figure 6. Concept representation of the vehicle in the sliding mode

Where y is the linear displacement of the upper part of the vehicle in m, φ is the inclination angle in degrees, m is the mass of only the upper part of the vehicle in Kg, F_L is the force of the linear motor in N. The mass m of the upper part includes the mass of the motors, batteries and the rider.

Using equation (1), the Lagrange function of the system can be expressed as follow:

$$L = \frac{m\dot{y}^2}{2} - mgy \sin\varphi \tag{2}$$

This yields the following equation of motion representing the upper part dynamics during the sliding mode:

$$F_L = m\ddot{y} + mg \sin\varphi \tag{3}$$

The linear force from the actuator F_L needs to compensate for the inertial force $m\ddot{y}$ and the component of the gravitational force $mg \sin\varphi$ of the weight of the upper part. $\ddot{y}$ represents the linear acceleration of the upper part of the vehicle in response to the force developed by the linear actuator.

3.1.2 Stabilization Mode

The vehicle can be described schematically by three coordinates as shown in Figure 7; linear motion of the system in the Y direction, angular motion of the body about the rod on the Z direction (tilt angle θ), and angular motion of the body about the cart (base) on the Y direction (inclination angle φ). The system inputs are the motor force activating the sliding part of the vehicle, the torques driving the wheels and a disturbance force acting on the vehicle due to external impact or obstacles.

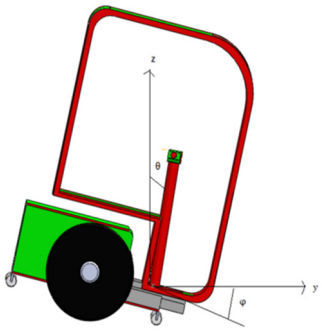

Figure 7. Schematic diagram of the TWMV with the rod

LE dynamic formulation on the vehicle during the stabilization mode yields the following equations:

$$\frac{\partial}{\partial t}\left(\frac{\partial L}{\partial \dot{Y}}\right)-\frac{\partial L}{\partial Y}=F_1 \tag{4}$$

$$\frac{\partial}{\partial t}\left(\frac{\partial L}{\partial \dot{\theta}}\right)-\frac{\partial L}{\partial \theta}=F_2 \tag{5}$$

Using equations (4) and (5), the systems equation of motion can be described as follows:

$$\left(M_c+m_r\right)\ddot{Y}-M_cL_c\left(\cos\left(\theta\right)+\sin\left(\theta\right)\right)\left(\ddot{\theta}+\dot{\theta}^2\right)=F_1 \tag{6}$$

$$\left(m_rL_r^2+M_cL_c^2\right)\ddot{\theta}+\left(m_rL_r\cos\left(\theta\right)-M_cL_c\sin\left(\theta\right)\right)\ddot{Y} + 2\left(M_cL_c^2-M_rL_r^2\right)g\cos\left(\theta\right)\sin\left(\theta\right)=F_2 \tag{7}$$

Where, Y is the linear displacement of the vehicle, θ is the tilt angle of the rod and the upright vertical Z axis, M_c is the mass of the cart including the mass of the motors and batteries, m_r is the mass of the rod including the mass of the rider, L_c is the distance from the centre of gravity to the centre of mass, L_r is the length of the rod, F_1 is the average driving force of the two wheel, and F_2 is an external disturbance force.

3.2 Linear Model

Linearization of the above non-linear 2nd order differential equations yields a linear model of the system in the state-space form.

$$\dot{X}=AX+Bu \tag{8}$$

$$Y=CX+Du \tag{9}$$

Where

A is the state matrix, B is the input matrix , C is the output matrix and D is the direct transmission matrix. The state space variables representing the dynamics of the vehicle can be expressed using the following state vector:

$$X=\begin{bmatrix} y & \theta & \varphi & \dot{y} & \dot{\theta} & \dot{\varphi} \end{bmatrix} \tag{10}$$

and the system linear equations can be expressed as follows where constants are described in the appendix:

$$\begin{bmatrix} \dot{x}_1 \\ \dot{x}_2 \\ \dot{x}_3 \\ \dot{x}_4 \\ \dot{x}_5 \\ \dot{x}_6 \end{bmatrix}=\begin{bmatrix} 0 & 0 & 0 & 1 & 0 & 0 \\ 0 & 0 & 0 & 0 & 1 & 0 \\ 0 & 0 & 0 & 0 & 0 & 1 \\ 0 & A_1 & A_4 & 0 & A_7 & A_{10} \\ 0 & A_2 & A_5 & 0 & A_8 & A_{11} \\ 0 & A_3 & A_6 & 0 & A_9 & A_{12} \end{bmatrix}\begin{bmatrix} x_1 \\ x_2 \\ x_3 \\ x_4 \\ x_5 \\ x_6 \end{bmatrix}+\begin{bmatrix} 0 & 0 \\ 0 & 0 \\ 0 & 0 \\ B_1 & 0 \\ B_2 & 1 \\ B_2 & 0 \end{bmatrix}\begin{bmatrix} F_1 \\ F_2 \end{bmatrix} \tag{11}$$

4. Control Approaches

4.1 PID Control

A schematic diagram of the system with the inputs and outputs is shown in Figure 8. The detailed control algorithm based on PID controllers is shown in Figure 9. According to the system design, the upper part has to slide, with constant angle of 18 degree, a distance of 15 cm before stopping at stage 3. Three PID controllers are considered where the parameters are adjusted manually. The same control approach is implemented on both the sliding mode

and stabilization mode. For this purpose, two switching mechanisms are designed to switch between the control algorithms on both modes.

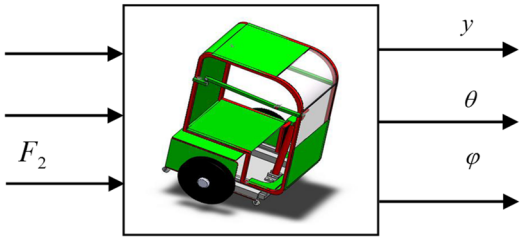

Figure 8. The system with inputs and outputs

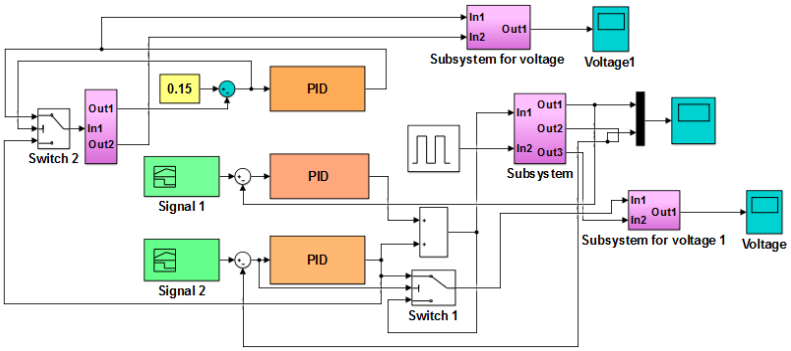

Figure 9. Schematic diagram of the control architecture

The control inputs are the 'error' and the derivative of 'error' for the three measured variables of the system: y, θ and φ represented by following equations:

$$e_{\partial_y} = \partial_{y_d} - \partial_{y_m} \qquad \dot{e}_{\partial_y} = \frac{d(e_{\partial_y})}{dt} \tag{12}$$

$$e_{\partial_\theta} = \partial_{\theta_d} - \partial_{\theta_m} \qquad \dot{e}_{\partial_\theta} = \frac{d(e_{\partial_\theta})}{dt} \tag{13}$$

$$e_{\partial_\varphi} = \partial_{\varphi_d} - \partial_{\varphi_m} \qquad \dot{e}_{\partial_\varphi} = \frac{d(e_{\partial_\varphi})}{dt} \tag{14}$$

The system response is analyzed in terms of the sliding displacement of the upper part, the tilt angle and the linear motion of the entire vehicle. The control effort, in terms of the motor voltage, is considered for the linear motor and the wheels' motors required to achieve the stabilization mode of the vehicle in the upright position. Results are represented in Figures 9 - 14. As the type of motion considered in this study is a linear forward/backward only, the two control signals from both the feedback loops are identical and hence the motor terminal voltage is a summation of both the voltage of the left and right wheels.

4.1.1 Sliding Mode of the Vehicle Moving Part (Transition from Stage 1 to Stage 2)

Controlling the upper part of the vehicle while sliding; transfer between stage 1 and stage 2, is achieved utilizing a PID control. Results of the motion are described in Figures 10 and 11. The upper part moved in a linear motion a distance 15 cm sliding over the base of the vehicle and reached the desired value in less than 5 seconds. A sudden change in the linear actuator voltage occurred at the period where the upper part stops as can be noticed in Figures 10 and 11.

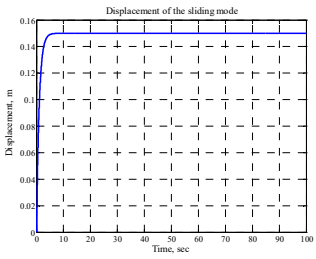

Figure 10. Sliding displacement

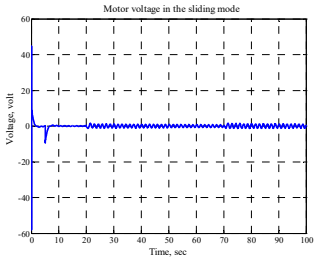

Figure 11. Linear motor voltage

4.1.2 Lifting Up and Stabilization (Transition from Stage 2 To Stage 3)

The system response during the stabilization mode is described in Figures 12, 13 and 14. The Linear displacement of the vehicle is described in Figure 10. The vehicle has to move from initial reference position a distance of 1.5 meters while keeping balance in the upright position. The controller achieved its target within around 7 seconds. The tilt angle is shown in Figure 12. The control effort required by the DC motor torque required to achieve the control target, described in Figure 14, tends to be high at the beginning of the motion and then decay until the system reaches stabilization after 10 seconds. It took the vehicle less than 10 seconds to move from rest for a distance 1.5 m in a linear motion as described in Figure 13.

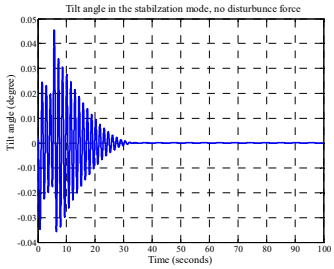

Figure 12. Tilt angle, no disturbamce

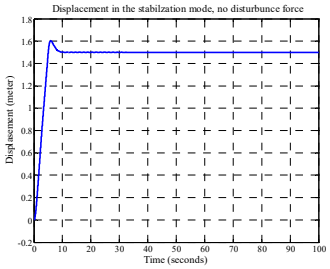

Figure 13. Linear disp., no disturbance

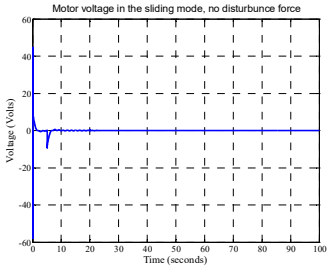

Figure 14. Stablization motor voltage

5. State Space Control

5.1 Linear Quadratic Regulator (LQR)

Linear Quadratic Regulator (LQR) is a state-space technique for designing optimal dynamic regulators. This technique refers to a linear system and a quadratic performance index according to the following equation;

$$\dot{X} = AX + Bu \tag{15}$$

The performance of a LQR system can be represented by an integral performance index in Equation 16. It enables a trade-off between regulation performance and control effort via the performance index when the initial state is predefined.

$$J = (x(t)^T Qx(t) + Ry(t)^2)dt \tag{16}$$

The control law for the LQR is specified as:

$$u = -R - B'Px \tag{17}$$

Where P = P′ ≥ 0 solves the following algebraic Ricatti equation

$$0 = PA + A'P - PBR - B'P + Q \tag{18}$$

The gain vector $K = R - B'P$ determines the amount of control feedback into the system. The matrix R and Q, will balance the relative importance of the control input and state in the cost function (J) being optimized with a condition that the elements in both Q and R matrices are positive values. The size of Q matrix depends on the size of the system's state matrix and R matrix is dependent on the number of control input to the system. The block diagram for the LQR controller is shown in Figure 15.

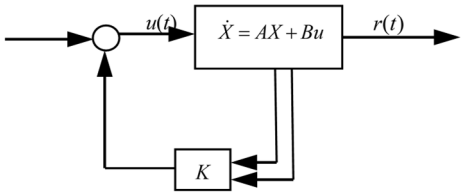

Figure 15. Block diagram of the LQR and poles placement control

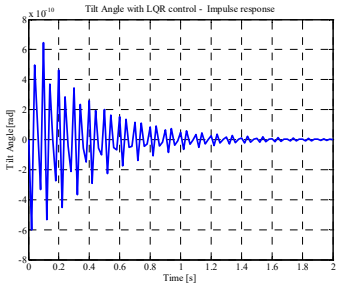

Figure 16. Tilt angle

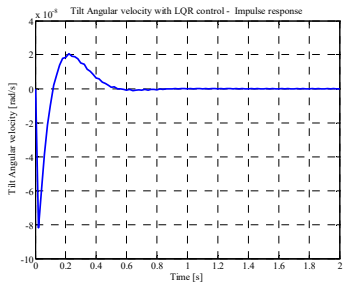

Figure 17. Angular velocity

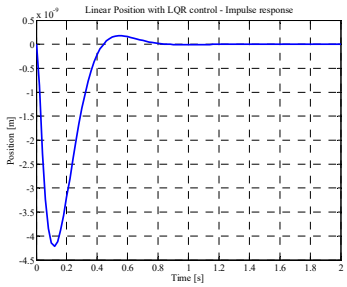

Figure 18. Linear displacement

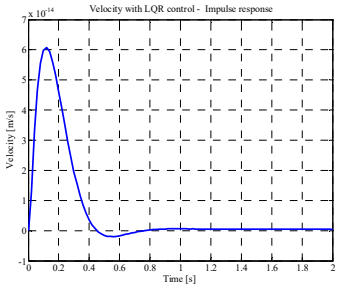

Figure 19. Vehicle linear velocity

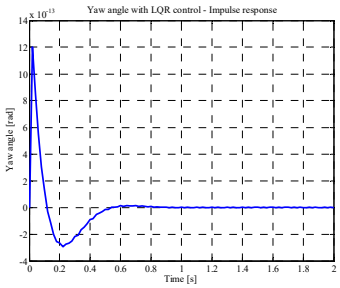

Figure 20. Vehicle yaw angle

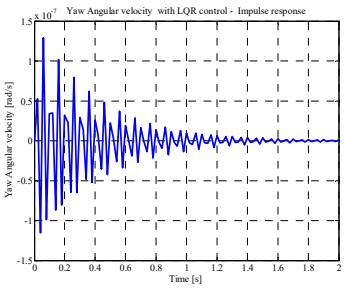

Figure 21. Derivative of the yaw angle

Results of the simulation for both the pole placement techniques and LQR are shown in Figures 16 - 21 and 25 - 27 respectively. For the pole placement technique, the system achieved the desired values; both the linear displacement and the tilt angle, in less than 1.5 seconds. The required control effort shown in Figure 27, measured in volts, is limited to 30 volts at the start while decay in respond to the developed control strategy.

5.1.1.1 Effect of Disturbance Force

A sudden impact force has applied at 2 seconds intervals on the vehicle body. The developed LQR has succeeded to a satisfactory level, shown in Figures 22 and 23, to absorb the impact disturbance while been able to bring back the vehicle to the desired vertical upright position. However, an occurrence of accumulated errors has been noticed in both the tilt angle and the linear displacement of the entire system. Increasing the time interval between each time the disturbance applies is recommended to avoid such occurrence.

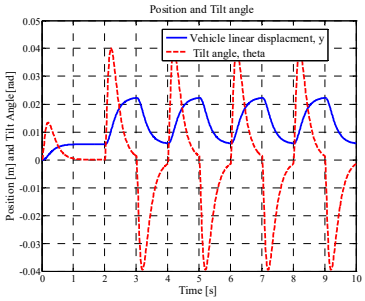

Figure 22. System performance

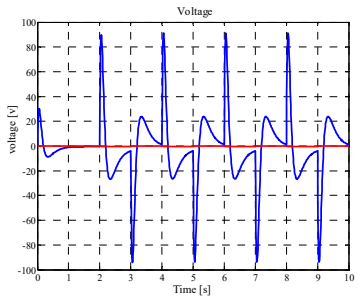

Figure 23. Control Output, volts

5.2 Pole Placement Results

The position of poles defines the stability of a system. According to linear control theory, the poles of the system can be arbitrarily placed in the complex plane if the controllability matrix is of full rank. The control law for the pole-placement controller is given as

$$u = -Kx \tag{19}$$

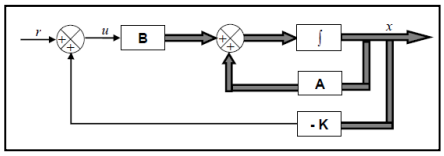

Figure 24. Block diagram for Pole-placement controller

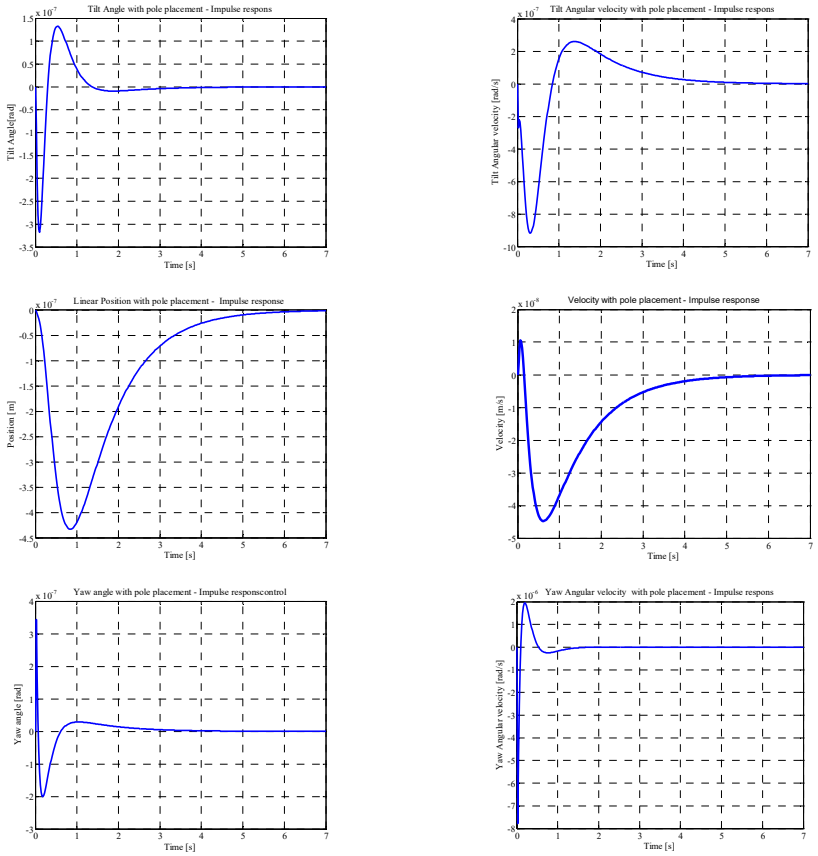

Figure 25. System performance with no disturbance

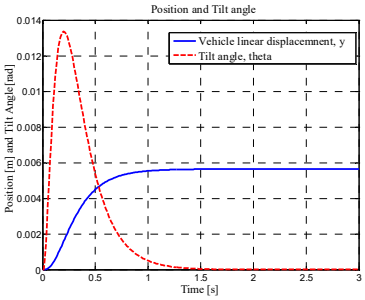

Figure 26. Tilt angle and linear displacement

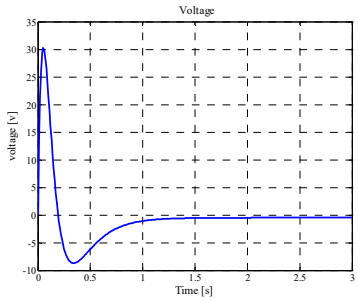

Figure 27. Control Output

where u is the control input, x is the state parameters and K is the state feedback gain matrix. Figure 24 shows the block diagram for the Pole-placement controller.

6. Conclusions

Mathmetical modelling of a new design of two-wheeled veicle has been presented along with a design and implementaion of a robust PID control strategy. The response of the system has been approved to be satisfactory. Measurement of the control effort for the entire motion of the vehicle (from stage 1 to stage 3) has been provided based on the developed PID control strategy. Modelling of the system has been presented based on Lagrangian - Euler formulation. The system has been simplified in three sucessive stages represention the sequence of the desired motion. The linearized state space model has been derived along with a design and implementaion of LQR as wel as pole placement techniques. The robustness of the LQR control scheme has been investigated based on the system response where there is an impact disturbance on the vehicle. Based on various simulation excerscises, the developed control showed reasonable robustness while having a smooth transition of the system between the various stages of operation.

References

Almeshalz, O., & Agouri, S. A. (2012). Mathematical Modelling And Pid Control of Squ-Two-Wheeled Mobility Vehicle (Squ-Twmv). In *Adaptive Mobile Robotics: Proceedings of the 15th International Conference on Climbing and Walking Robots and the Support Technologies for Mobile Machines, Baltimore, USA, 23-26 July, 2012* (p. 137-144). World Scientific. https://dx.doi.org/10.1142/97898 14415958_0021

Bogdanov, A. (2004). *Optimal Control of a Double Inverted Pendulum on a Cart*. Oregon Health and Science University Technical Report CSE.

Browning, B., Rybski, P. E., Searock, J., & Veloso, M. M. (2004, April). Development of a soccer-playing dynamically-balancing mobile robot. In *Robotics and Automation, 2004. Proceedings. ICRA'04. 2004 IEEE International Conference on* (Vol. 2, pp. 1752-1757). IEEE. https://dx.doi.org/10.1109/robot.2004.1308077

Bugeja, M. (2003, September). Non-linear swing-up and stabilizing control of an inverted pendulum system. In *EUROCON 2003. Computer as a Tool. The IEEE Region 8* (Vol. 2, pp. 437-441). IEEE. https://dx.doi.org/10.1109/eurcon.2003.1248235

Fiacchini, M., Viguria, A., Cano, R., Prieto, A., Rubio, F. R., Aracil, J., & Canudas-de-Wit, C. (2006, September). Design and experimentation of a personal pendulum vehicle. In *Proc. Seventh Portuguese Conf. Automatic Control*.

Goher, K. M., & Tokhi, M. O. (2008). Balance control of a TWRM with a static payload. In *Proceedings of the 11th International Conference on Climbing and Walking Robots and the Support Technologies for Mobile Machines (CLAWAR 2008)*. Coimbra, Portugal, September 8-10. https://dx.doi.org/10.1142/9789812835772_0004

Han, H., & Qiao, J. (2010). A self-organizing fuzzy neural network based on a growing-and-pruning algorithm. *IEEE Transactions on Fuzzy Systems*, *18*(6), 1129-1143. https://dx.doi.org/10.1109/TFUZZ.2010.2070841

Harrison, R. F. (2003). Asymptotically optimal stabilising quadratic control of an inverted pendulum. *IEE Proceedings-Control Theory and Applications*, *150*(1), 7-16. https://dx.doi.org/10.1049/ip-cta:20030014

Li, J., Gao, X., Huang, Q., & Matsumoto, O. (2008, August). Controller design of a two-wheeled inverted pendulum mobile robot. In *2008 IEEE International Conference on Mechatronics and Automation* (pp. 7-12). IEEE. Retrieved from http://posgrado.itlp.edu.mx/aduarte/desing_control_pendulum.pdf

Lin, Z., Saberi, A., Gutmann, M., & Shamash, Y. (1996). Linear controller for an inverted pendulum having restricted travel-a high-and-low gain approach. *Automatica, 32*, 933-937. http://dx.doi.org/10.1016/0005-1098(96)00006-4

Nasir, A., Ahmad, M., & Ismail, R. R. (2010). The control of a highly nonlinear two-wheels balancing robot: A comparative assesment between linear quadratic regulator (LQR) and PID control schemes. *International Science Index*, *4*(10), 330-331.

Nawawi, S. W., Ahmad, M. N., & Osman, J. H. S. (2006, September). Control of two-wheels inverted pendulum mobile robot using full order sliding mode control. In *Proceedings of International Conference on Man-Machine Systems* (pp. 15-16). Retrieved from https://www.scribd.com/document/92038586/Control-of-Two-wheels-Inverted-Pendulum-Mobile-Robot-Using-Full-Order-Sliding-Mode-Control

Salerno, A., & Angeles, J. (2004). The control of semi-autonomous two-wheeled robots undergoing large payload-variations. In *Robotics and Automation, 2004. Proceedings. ICRA'04. 2004 IEEE International Conference on* (Vol. 2, pp. 1740-1745). IEEE. http://dx.doi.org/10.1016/S0005-1098(01)00174-1

Salerno, A., & Angeles, J. (2004, June). The control of semi-autonomous self-balancing two-wheeled quasiholonomic mobile robots. In *Proc. of the 15th CISM-IFToMM Symposium on Robot Design, Dynamics and Control (RoManSy)*.

Tatikonda, R. C., Battula, V. P., & Kumar, V. (2010, May). Control of inverted pendulum using adaptive neuro fuzzy inference structure (ANFIS). In *Proceedings of 2010 IEEE International Symposium on Circuits and Systems* (pp. 1348-1351). IEEE. http://dx.doi.org/10.1109/ISCAS.2010.5537234

Tinkir, M., Kalyoncu, M., Onen, U., & Botsali, F. M. (2010, February). PID and interval type-2 fuzzy logic control of double inverted pendulum system. In *Computer and Automation Engineering (ICCAE), 2010 The 2nd International Conference on* (Vol. 1, pp. 117-121). IEEE. http://dx.doi.org/10.1109/ICCAE.2010.5451988

Tokhi, M. O., & Almeshalz, A. M. (2012). State Space Modelling and Control of SQU-Two-Wheeled Mobility Vehicle (SQU-TWMV): An Energy Analysis Approach. In *Adaptive Mobile Robotics: Proceedings of the 15th International Conference on Climbing and Walking Robots and the Support Technologies for Mobile Machines, Baltimore, USA, 23-26 July, 2012* (p. 55-62). World Scientific. https://dx.doi.org/10.1142/9789814415958_0011

Vermeiren, L., Dequidt, A., Guerra, T. M., Rago-Tirmant, H., & Parent, M. (2011). Modeling, control and experimental verification on a two-wheeled vehicle with free inclination: an urban transportation system. *Control Engineering Practice*, *19*(7), 744-756. http://dx.doi.org/10.1016/j.conengprac.2011.04.002

Wongsathan, C., & Sirima, C. (2009, February). Application of GA to design LQR controller for an Inverted Pendulum System. In *Robotics and Biomimetics, 2008. ROBIO 2008. IEEE International Conference on* (pp. 951-954). IEEE. http://dx.doi.org/10.1109/ROBIO.2009.4913127

Xiong, X., & Wan, Z. (2010, July). The simulation of double inverted pendulum control based on particle swarm optimization LQR algorithm. In *2010 IEEE International Conference on Software Engineering and Service Sciences* (pp. 253-256). IEEE. http://dx.doi.org/10.1109/ICSESS.2010.5552427

Appendix

$$
\begin{aligned}
A_1 = {} & \left(F_1 \sin(x_2)/L_r - 2L_r m_r g \cos(x_2^3) + 4L_r m_r g \sin(x_2^2)\cos(x_2) + L_r m_r \cos(x_2) x_5^2\right) \\
& /\left(1 - m_r \cos(x_2^2) - M_c \sin(x_3^2)\right)/\left(m_r + M_c\right) - 2\left(F_1\left(1 - \cos(x_2)/L_r + \sin(x_3)/L_c\right)\right. \\
& - 2L_r m_r g \sin(x_2)\cos(x_2^2) + M_c L_c \cos(x_3) x_6^2 - 2M_c L_c g \cos(x_3)\sin(x_3^2) + L_r m_r \sin(x^2) x_5^2\Big) \\
& /\left(1 - m_r \cos(x_2^2) - M_c \sin(x_3^2)\right)^2 /\left(m_r + M_c\right) m_r \cos(x_2)\sin(x_2)
\end{aligned}
$$

$$
\begin{aligned}
A_2 = {} & -2L_r^2 \sin(x_2^2) m_r g + 2L_r^2 \cos(x_2^2) m_r g + 1/L_r \sin(x_2)\sin(x_2)(F_1(1-\cos(x_2)/L_r + \sin(x_3)/L_c) \\
& 2L_r m_r g \sin(x_3)\cos(x_3^2) + M_c L_c \cos(x_3) x_6^2 - 2M_c L_c g \cos(x_3)\sin(x_3^2) \\
& + L_r m_r \sin(x_2) x_5^2)/(1 - m_r \cos(x_2^2) - M_c \sin(x_3^2))/(m_r + M_c) - 1/L_r \cos(x_2)(F_1 \sin(x_2)/L_r \\
& + L_r m_r \cos(x_2) x_5^2)/(1 - m_r \cos(x_2^2) - M_c \sin(x_3^2)/(M_c + m_r) \\
& + 2/L_r \cos(x_2^2)(F_1(1-\cos(x_2)/L_r + \sin(x_3)/L_c)) - 2L_r m_r g \sin(x_3)\cos(x_3^2) + M_c L_c \cos(x_6^2) \\
& - 2M_c L_c g \cos(x_3)\sin(x_3^2) + L_r m_r \sin(x_2) x_5^2)/(1 - m_r \cos(x_2^2) - M_c \sin(x_3^2))^2/(M_c + m_r) m_r \sin(x_2)
\end{aligned}
$$

$$A_3 = 1/L_c \sin(x_3)(F_1 \sin(x_2)/L_r - 2L_r m_r g \cos(x_2^3) + 4L_r m_r g \sin(x_2^2)\cos(x_2) + L_r m_r \cos(x_2) x_5^2)/(1 - m_r \cos(x_2^2) - M_c \sin(x_3^2))/(m_r + M_c) - 2/L_c \sin(x_3)(F_1(1-\cos(x_2)/L_r + \sin(x_3)/L_c) - 2L_r m_r \sin(x_2)\cos(x_2^2) + L_c M_c \cos(x_3) x_6^2) - 2M_c L_c g \cos(x_3)\sin(x_3^2) + L_r M_r \sin(x_2) x_5^2)/(1 - m_r \cos(x_2^2)) - M_c \sin(x_3^2))^2/(m_r + M_c) m_r \cos(x_2)\sin(x_2)$$

$$A_4 = (F_1 \cos(x_3)/L_c - M_c L_c \sin(x_3) x_6^2 + 2M_c L_r g \sin(x_3^3) - 4M_c L_r g \sin(x_3)\cos(x_3^2))/(1 - m_r \cos(x_2^2)) - M_c \sin(x_3^2)/(m_r - M_c) + 2(F_1(1-\cos(x_2)/L_r) + \sin(x_3)/L_c) - 2/L_c \sin(x_3)(F_1(1-\cos(x_2)/L_r + \sin(x_3)/L_c) - 2L_r m_r \sin(x_2)\cos(x_2^2) + L_c M_c \cos(x_3) x_6^2 - 2M_c L_c g \cos(x_3)\sin(x_3^2) + L_r M_r \sin(x_2) x_5^2)/(1 - m_r \cos(x_2^2)) - M_c \sin(x_3^2))^2/(m_r + M_c) M_c \cos(x_3)\sin(x_3)$$

$$A_5 = -1/L_r \cos(x_2)(F_1 \cos(x_3)/L_c - 2L_r m_r g \cos(x_3^3) + 4L_r m_r g \sin(x_3^2)\cos(x_3) - M_c L_c \sin(x_3) x_6^2 + 2L_c M_c g \sin(x_3^3) + 4M_c L_c g \cos(x_3^2)\sin(x_3))/(1 - m_r \cos(x_2^2)) - M_c \sin(x_3^2))/(m_r + M_c) - 2/L_r \cos(x_2)(F_1(1-\cos(x_2)/L_r + \sin(x_3)/L_c) - 2L_r m_r g \sin(x_3)\cos(x_3^2) + M_c L_c \cos(x_3) x_6^2 - 2M_c L_c g \cos(x_3)\sin(x_3^2) + L_r m_r \sin(x_2) x_5^2)/(1 - m_r \cos(x_2^2) - M_c \sin(x_3^2))^2/(M_c + m_r) M_c \sin(x_3)\cos(x_3)$$

$$A_6 = -2L_c^2 \cos(x_3^2) M_c g + 2L_c^2 \sin(x_3^2) M_c g + 1/L_c \cos(x_2)\sin(x_2)(F_1(1-\cos(x_2)/L_r + \sin(x_3)/L_c) - 2L_r m_r g \sin(x_2)\cos(x_2^2) + M_c L_c \cos(x_3) x_6^2 - 2M_c L_c g \cos(x_3)\sin(x_3^2) + L_r m_r \sin(x_2) x_5^2)/(1 - m_r \cos(x_2^2) - M_c \sin(x_3^2))/(m_r + M_c) - 1/L_c \sin(x_2)(F_1 \cos(x_2)/L_c - L_c M_c \sin(x_3) x_6^2) + 2M_c L_c g \sin(x_3^3) + 4L_c M_c g \cos(x_3^2)\sin(x_3))/(1 - m_r \cos(x_2^2) - M_c \sin(x_3^2)/(m_r + M_c) + 2/L_c \sin(x_3^2)(F_1(1-\cos(x_2)/L_r + \sin(x_3)/L_c - 2M_r L_r g \sin(x_2)\cos(x_2^2) + M_c L_c \cos(x_3) x_6^2 - 2L_c M_c g \cos(x_3)\sin x_3^2) + L_r m_r \sin(x_2) x_5^2)/(1 - m_r \cos(x_2^2) - M_c \sin(x_3^2)^2/(m_r + M_c) M_c \cos(x_3)$$

$$A_7 = 2L_r m_r \sin(x_2) x_5/(1 - m_r \cos(x_2^2) - M_c \sin(x_3^2)/(m_r + M_c)$$

$$A_8 = -2m_r \cos(x_2)\sin(x_5)/(1 - m_r \cos(x_2^2) - M_c \sin(x_3^2)/(m_r + M_c)$$

$$A_9 = 2/L_c L_r m_r \sin(x_2)\sin(x_3) x_5/(1 - m_r \cos(x_2^2) - M_c \sin(x_3^2)/(m_r + M_c)$$

$$A_{10} = 2L_c M_c \cos(x_3) x_6/(1 - m_r \cos(x_2^2) - M_c \sin(x_3^2)/(m_r + M_c)$$

$$A_{11} = -2/L_r L_c M_c \cos(x_3) x_6/(1 - m_r \cos(x_2^2) - M_c \sin(x_3^2)/(m_r + M_c)$$

$$A_{12} = 2M_c \sin(x_3)\cos(x_3) x_6/(1 - m_r \cos(x_2^2) - M_c \sin(x_3^2)/(m_r + M_c)$$

$$B_1 = (1 - \cos(x_2)/L_r + \sin(x_3)/L_c)/(1 - m_r \cos(x_2^2) - M_c \sin(x_3^2)/(m_r + M_c)$$

$$B_2 = -1/L_r \cos(x_2)(1 - \cos(x_2)/L_r + \sin(x_3)/L_c)/(1 - m_r \cos(x_2^2) - M_c \sin(x_3^2)/(m_r + M_c)$$

$$B_3 = 1/L_c \sin(x_3)(1 - \cos(x_2)/L_r + \sin(x_3)/L_c)/(1 - m_r \cos(x_2^2) - M_c \sin(x_3^2)/(m_r + M_c)$$

Copyrights